Building and Environment 93 (2015) 1–8

Contents lists available at ScienceDirect

Building and Environment

journal homepage: www.elsevier.com/locate/buildenv

Acoustic performance of balconies having inhomogeneous ceiling surfaces on a roadside building facade

Xu Wang, Dongxing Mao*, Wuzhou Yu, Zaixiu Jiang

Institute of Acoustics, Tongji University, No. 1239 Siping Road, Shanghai 200092, China

ARTICLE INFO

Article history:
Received 29 March 2015
Received in revised form
24 June 2015
Accepted 26 June 2015
Available online 4 July 2015

Keywords:
Balcony
Insertion loss
Inhomogeneous impedance surface

ABSTRACT

Balconies provide noise screening effects in residential buildings even with the balcony door opened for natural ventilation. However, the screening effect of a balcony was found to be canceled due to the reflection from the ceiling. This paper describes a balcony whose ceiling is made from materials of inhomogeneous impedance which eliminates this drawback. The nonuniform impedance affects wave behavior by altering the direction of energy flux away from the region of a balcony as it reflects on the ceiling. A proposed realization of the balcony ceiling comprises a closely spaced array of progressively tuned hollow narrow tubes which create a phase gradient. The acoustic performance of a balcony with an inhomogeneous ceiling surface is examined theoretically by a ray-based model. All of the results predicted by the theory fit well with numerical simulations using a two-dimensional finite element method. Balconies with the proposed ceilings have the potential to be widely used in a roadside multi-residential building against the exterior traffic noise.

1. Introduction

Balconies are architectural features functioned as a buffer zone to provide a comfortable environment for residents, and recently regarded as one of the green and innovative features in residential building [1]. Due to the high density of population and the scarcity of building land in metropolis, it is common that multi-residential buildings are located close or even next to traffic roads and hence exposed to severe exterior noise. Existing sound protecting treatments, such as sound barriers, are limited in their ability to protect a roadside building, especially the upper stories, against the road traffic noise [2]. However, balconies were found to be effective in providing the noise screening effect in residential blocks even with the balcony door opened for natural ventilation [3]. Therefore, there have been a diversity of studies on investigating the screening effect of balconies. Mohsen and Oldham [4] investigated a closed balcony by computer simulation and measurements on a scale model, and derived an empirical equation to predict the performance of a closed balcony. May [5] observed a significant increase in sound level on high-rise balconies close to freeways by field measurement, and the sound absorption treatment of the ceiling was found to provide effective noise reduction. Boundary element method (BEM) was also used to study the performance of balconies in a tall building close to a road [6]. Kim et al. [7] investigated a special type of balcony, i.e. balconies fitted with windows, by using in-situ measurement. To predict the sound field inside balconies, which are partially covered by absorptive materials, Kropp and Berillon [8] developed a theoretical model by using the Green's function for rigid walls and replacing the non-rigid areas by monopole sources. Cheng et al. [9] carried out a theoretical study on windows with lintels, which are structures similar to balconies, by combining Macdonald's diffraction theory and the image receiver method. As a modification of the standard prediction scheme CRTN [10], a methodology based on the geometrical ray theory was developed for the prediction of sound field inside a balcony [11]. Furthermore, the form of balcony was also attracted much attention: A balcony opened to the street but enclosed on all other sides was investigated by means of scale models by Hammad et al. [12]. Hossam El-Dien and Woloszyn [13,14] tested the influence of balcony configurations, which include the ceiling inclined angle, balcony depth and parapet form, on the acoustic performance of building facades close to roadways using pyramid tracing simulations and scale model measurements. In addition, a study on the scattering effects of balconies has also been carried out using a scale model [15]. The studies mentioned above defined exterior noises solely as traffic noise and considered the balcony effect on a single

* Corresponding author.
E-mail address: dxmao@tongji.edu.cn (D. Mao).

http://dx.doi.org/10.1016/j.buildenv.2015.06.027
0360-1323/

building, Lee et al. [16] then investigated the noise reduction of balconies in an apartment complex and took other noises such as those produced from vehicles entering and exiting a parking lot or from nearby outdoor market into consideration.

When a multi-residential building is located near a road, the screening effect provided by a balcony declines for the occurrence of reflection from the ceiling [6,9]. In continuing efforts to improve the performance of balconies, a diversity of studies on various balcony forms have been conducted [12–15]. Nonetheless, the profiles of these types of balconies are relative complex. On the other hand, active noise control (ANC) has been used to reduce the amount of sound diffracted at the edge of balconies [17]. In particular, sound absorptive treatment was found to be very effective in counteracting the degradation due to the reflection from the ceiling [6]. However, because of the accumulation of dust and bacteria, the requirement of fireproof, as well as the irritation of human respiration system due to fibers from porous materials, the existing absorptive materials are not suitable for longterm use in practice. Moreover, using available absorptive materials leads to impractically thick balcony for low frequency absorption.

In the present study, we seek for a potential alternative solution—barriers whose ceilings having inhomogeneous surfaces—to improve the shielding effect of balconies in a road-side buildings. The balcony ceiling has a simple profile like that of a conventional rigid wall. By introducing an impedance inhomogeneity [18,19], the way the sound behaves as it reflects on the ceiling is altered. Balconies having ceilings with inhomogeneous surfaces successfully guide the sound energy flux away from the region of a balcony, and hence provide a better noise screening effect. In Sec. 2 of this paper, a balcony with a conventional rigid-wall ceiling is investigated theoretically and numerically. In Sec. 3, the behavior of sound interacting with an inhomogeneous impedance surface is evaluated; then the theoretical analysis and numerical simulations on the performance of a balcony having an inhomogeneous ceiling surface are carried out. Finally, a physical example of an inhomogeneous ceiling surface is demonstrated in Sec. 4.

2. Balconies with rigid-wall ceilings

2.1. Theoretical analysis

In this section, the first treatment—a balcony with a conventional ceiling (i.e. rigid-wall ceiling)—is considered, which is the most common case in practical use. Fig. 1 shows the cross sections (in the x–y plane) of a multi-residential building placed very close to a source on the ground; and the geometries are listed in the figure caption. This investigated model is equivalent to an infinite coherent line source parallel to a high building with a constant cross-section facade in three dimensions. Therefore, for the current analysis, the contributions of sound diffraction from the top edge of the facade and the vertical edges of the balconies are ignored. For clarity, the front parapet of each balcony is assumed to be acoustically transparent and will not be shown in the following figures. Notice that it is a critical circumstance since the source is placed very close to the building facade. Nonetheless, using the theoretical approach adopted in this paper, it is straightforward to study the performance of balconies with different source locations. For this conventional treatment, the ground, as well as the ceiling and back wall of each balcony are assumed to be rigid.

In this paper, a ray-based theory, which combines the image receiver method [9,11] and the theory of sound diffraction [20,21], is used to investigate the performance of a balcony. When a road-side multi-residential building is located close to a noise source, as shown in Fig. 1 with the given geometrical configuration, the

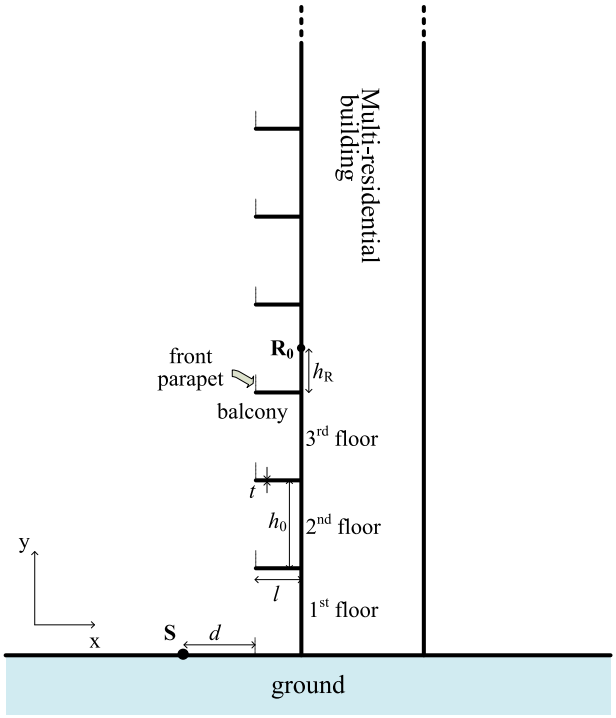

Fig. 1. Schematic representation of a multi-residential building located close to a source. $d = 2.5\ m$, $l = 1.5\ m$, $t = 0.1\ m$, $h_0 = 3\ m$, $h_R = 1.5\ m$.

receiver $\mathbf{R_0}$ is shielded from the source **S** by the balcony (i.e. is located in the shadow zone). Thus, the total sound pressure at $\mathbf{R_0}$ with the presence of the balcony can be obtained by combining contributions of the reflected ray and all diffracted rays, as

$$p_w = p_{reflect} + p_{diffract} \tag{1}$$

where $p_{reflect}$ represents the contribution of the ray that is generated from the source **S**, and then experiences multiple reflections from the ceiling and floor of the balcony on the 4th story before it reaches the receiver $\mathbf{R_0}$. The term, $p_{diffract}$, represents the overall contributions from the diffracted rays, which leave the source, diffract at the edge $\mathbf{E_1}$ or $\mathbf{E_2}$, and then experience reflections with different orders before reaching $\mathbf{R_0}$. For these diffracted rays, as illustrated in Fig. 2(a) and (b), the row of image receivers of the receiver $\mathbf{R_0}$ can be readily created by using a simple ray tracing technique. Then the ray path from the source to the corresponding image receiver is constructed by linking the source and receiver. For instance, an image receiver $\mathbf{R_1}$ is created for the ray that diffracts at $\mathbf{E_1}$ (the edge of the balcony floor) and then hits the balcony ceiling before it reaches $\mathbf{R_0}$. The image receiver $\mathbf{R_2}$ creates the ray that diffracts at $\mathbf{E_1}$, hits the ceiling, and then the balcony floor before it reaches $\mathbf{R_0}$. In an analogous manner, the ray paths traced by other image receivers, $\mathbf{R_3}$, $\mathbf{R_4}$, and so on, can be straightforwardly determined. These image receivers with positive subscripts correspond to the diffracted rays diffracted by the edge of the balcony floor, while other image receivers with negative subscripts are corresponding to the sound rays diffracted at the edge of the ceiling. For the reflected ray, the corresponding image receiver can be readily determined by using the same ray tracing technique. As illustrated in Fig. 2(a), the image receiver for the reflected ray is $\mathbf{R_2}$, which is the same virtual receiver for the diffracted ray of order 2 mentioned above. For the current investigated model, by setting the location of the actual receiver $\mathbf{R_0}$ as the origin, the vertical locations of these image receivers $\mathbf{R_n}$ ($n = \pm 1, 2, 3, \ldots$) are given by

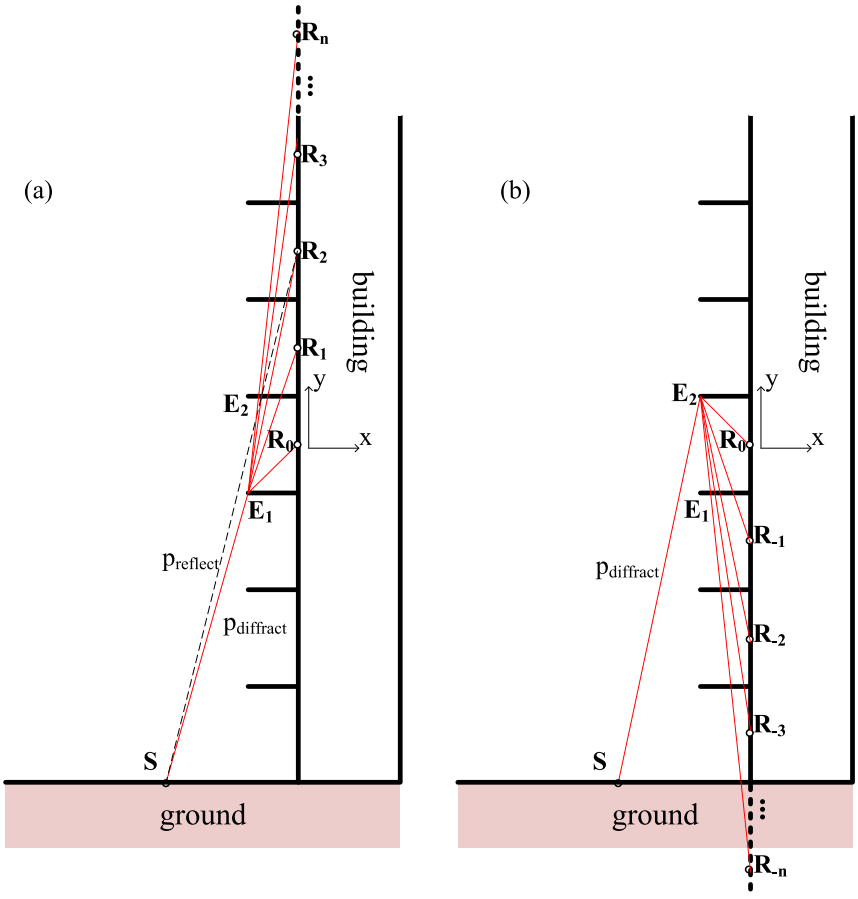

Fig. 2. Schematic diagram of the image receivers corresponding to (a) the reflected ray and the diffracted rays diffracted by the edge of the balcony floor and (b) the diffracted rays diffracted by the edge of the balcony ceiling.

$$y_n = \begin{cases} sign(n)\left[(|n|+1)h_0 - 2h_{(n)}\right] & \text{if } n \text{ is odd} \\ nh_0 & \text{if } n \text{ is even} \end{cases} \tag{2}$$

where $h_{(n)} = h_R$ for the image receivers with positive n, while $h_{(n)} = h_0 - h_R$ for those with $n < 0$. And $sign(n)$ is the sign function. In Eq. (2), the absolute value of n represents the number of reflection that the diffracted or reflected ray experiences before reaching $\mathbf{R_0}$ (also called the order of the ray). Notice that there is a ray that diffracts at $\mathbf{E_1}$ and then reaches $\mathbf{R_0}$ directly. Similarly, another ray, which is diffracted by $\mathbf{E_2}$ before reaching $\mathbf{R_0}$, exists. Both of these diffracted rays are of order zero; and the corresponding receiver is $\mathbf{R_0}$. In general, the paths linking the source and the receivers for the reflected and diffracted rays are shown by the dotted and solid lines in Fig. 2, respectively. For clarity, the image sources correspond to the reflected ray and those diffracted rays diffracted at $\mathbf{E_1}$ are shown in Fig. 2(a), and the image sources correspond to the diffracted rays diffracted by $\mathbf{E_2}$ are shown in Fig. 2(b).

As illustrated in Fig. 2(a) and (b), there are infinite number of image receivers. However, previous works [9,10] on balconies generally considered the contributions from the diffracted rays up to the first order, and the contributions of sound diffractions from the balcony ceiling were usually ignored. These may provide predictions with acceptable accuracy in most situations, but will lead to significant deviation when a building is placed very close to a road. Theoretically, the pressure at the receiver $\mathbf{R_0}$ is determined by the reflected ray and a coherent summation of contributions from all diffracted rays as they reaches the receivers $\mathbf{R_n}$ ($n = 0, \pm1, \pm2, \ldots$). However, for the calculation efficiency, only a finite number of image sources are considered. In the investigation on similar structures – parallel barriers, it has been reported that the variation of total sound pressure at the actual receiver $\mathbf{R_0}$ as a function of the number of reflection stabilized after 15 reflections [22]. So the image sources taken into account in present study are up to order 15 ($|n| \leq 15$).

In this paper, the diffraction theory [20,21] is combined with the image receiver method to investigate the performance of a roadside balcony. Pierce [21] has developed a solution to the wave equation for sound diffracted by a rigid-wall screen with edge $\mathbf{E}$ for a line source $\mathbf{S}$ and receiver $\mathbf{R_n}$. It is given by Ref. [21].

$$p_{diffract,n} = \left(\frac{e^{j\frac{\pi}{4}}}{\sqrt{2}}\right)\left[A_D(X_{+,n}) + A_D(X_{-,n})\right]\left[-jH_0^{(1)}(kr_n)\right] \tag{3}$$

where

$$r_n = r_S + r_{R,n} \tag{4}$$

The terms, r_S and $r_{R,n}$, are the respective distances from the source $\mathbf{S}$ and receiver $\mathbf{R_n}$ to the diffraction point $\mathbf{E}$, k is the wave number, and $H_0^{(1)}$ is the Hankel function of first kind and order zero. A_D is the Airy function [23] given by

$$A_D(X) = sign(X)[f(|X|) - jg(|X|)] \tag{5}$$

where $sign(X)$ is the sign function, and f and g are the auxiliary Fresnel functions [23]. The diffraction integrals, $X_{+,n}$ and $X_{-,n}$, are determined by

$$X_{\pm,n} = X(\theta_{R,n} \pm \theta_S) \tag{6}$$

where

$$X(\theta) = \left[-2\cos\left(\frac{\theta}{2}\right)\right]\sqrt{\frac{2r_S r_{R,n}}{\lambda r_n}} \tag{7}$$

where λ is the wavelength, and the angles, $\theta_{R,n}$ and θ_S, are illustrated in Fig. 3.

For a reflected ray that experiences multiple reflections before it reaches the receiver $\mathbf{R_0}$, as shown by the dashed line in Fig. 2(a), the contribution to the total sound field is given as [20].

$$P_{reflect} = -jH_0^{(1)}(kr_0) \tag{8}$$

where r_0 is the distance from the source **S** to the corresponding image receiver $\mathbf{R_2}$, and $H_0^{(1)}$ is the Hankel function of first kind and order zero. In this paper, the insertion loss (IL) is used to access the acoustic performance of a balcony, which is defined as follows:

$$IL = 20\log_{10}\left(\frac{P_{w/o}}{P_w}\right) \tag{9}$$

which is the decibel value of the ratio of sound pressure at $\mathbf{R_0}$ without ($P_{w/o}$) and with (P_w) the presence of a balcony.

2.2. Comparison with numerical simulations

A two-dimensional finite element method (FEM) was performed by employing the commercial software COMSOL Multiphysics™ to verify the theoretical analysis for the conventional treatment (i.e. a balcony with a rigid-wall ceiling). The calculation domain is shown in grey in Fig. 4. All surfaces, including the ceiling, floor and real wall of each balcony, as well as the ground are assumed to be rigid. In the present study, the domain of the radiated sound field extends to infinity; however, for computational efficiency, a relatively small area is considered for the numerical calculations. For this case, the calculation domain is bounded by perfectly matched layers (PMLs), which are artificial absorbing layers allowing waves to propagate out from the domain without reflection [24]. In other words, PMLs are added to the calculation domain to mimic the open domain of the radiated sound field. The PMLs are shown in Fig. 4, and for simplicity they are not shown in the following figures. The frequency range of interest is taken to be 200–4000 Hz. To ensure numerical accuracy, a fine mesh was used to divide the model into more than 370,000 triangular elements whose dimensions were kept below 0.02 m.

Fig. 5(a) shows the comparison of the IL curve predicted by the ray-based method with the FEM simulation results. The general trend of the IL curve such as the position of the peaks and dips predicted by the ray-based method coincides well with those FEM results in the whole frequency range of interest. As shown in Fig. 5(a), the conventional treatment, which was with a rigid-wall ceiling, made the sound attenuation performance of a balcony

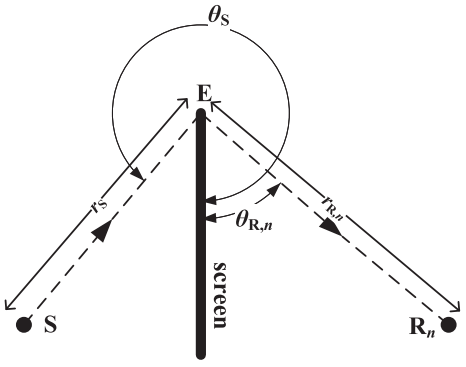

Fig. 3. The geometrical configuration for the diffraction of sound by a screen.

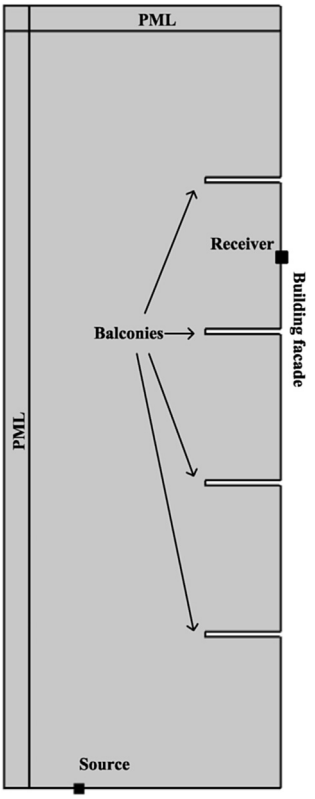

Fig. 4. The finite element modeling of balconies with rigid-wall ceilings in a roadside building.

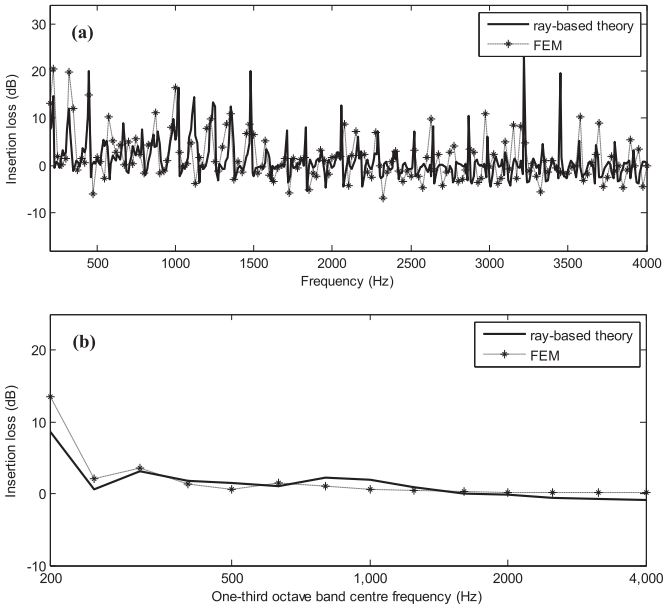

Fig. 5. (a) The spectrum of insertion losses at the receiver $\mathbf{R_0}$ for the case of a balcony with a rigid-wall ceiling. (b) Insertion losses in one-third octave band centre frequency.

worse at some frequencies (see those IL values below zero). The comparison of IL curves in 1/3 octave band is shown in Fig. 5(b), which also exhibits well agreement between these two methods. As illustrated in Fig. 5(b), when a source is located very close to a building, the shielding effect provided by a balcony is largely canceled due to the reflection from the conventional ceiling. Only at low frequencies (200–250 Hz), a balcony with the conventional ceiling has a noticeable effect on reducing the exterior noise. At most of the frequencies of interest (250–4000 Hz), both the insertion losses predicted theoretically and numerically are around zero. The overall IL, predicted by the ray-based theory and FEM simulations, are only 0.8 and 0.5 dB respectively, which means that the conventional treatment provides little effect on protecting a building against nearby traffic noise.

3. Balconies having inhomogeneous ceiling surfaces

3.1. Manipulation of a wavefront using a surface of inhomogeneous impedance

To overcome the degradation due to the reflection from the conventional ceiling, in this section, the second treatment—a balcony whose ceiling has inhomogeneous impedance surface—is proposed. In this case, the proposed ceiling (i.e. ceiling with an inhomogeneous surface) works by manipulating the behavior of sound reflection on its surface. Therefore, in this section, the methodology of wavefront manipulation based on the surface impedance inhomogeneity is introduced first. The following sets out how the wavefront of a reflected wave can be manipulated by introducing impedance variations of the surface. The phenomenon can be described by the generalized law of reflection [18], which was originally discovered in optics and then introduced to acoustics [19]. However, for the sake of completeness, a brief description of this theory is required here. As shown in Fig. 6, when sound reflects at a boundary, the trajectory from point **A** to point **B** has stationary phase (a result identical to Fermat's principle in optics [25]). This means that sound rays traveling close to the actual reflection path will arrive nearly in-phase and so reinforce each other.

Consider now that the impedance of the boundary is no longer homogeneous but shifts over the scale of a wavelength along the reflection path. In Fig. 6, if the two reflection paths are assumed to be in the vicinity of the actual path, then their phase difference at the point **B** is zero. Therefore, the phase difference of the two paths is given as [18,19].

$$[k\sin(\theta_i)dx + (\phi + d\phi)] - [k\sin(\theta_r)dx + \phi] = 0\,, \tag{10}$$

where k is the wave number of sound in air; θ_i and θ_r denote the angles of incidence and reflection; dx is the distance between the nearby points at x and $x + $ dx; and ϕ and $\phi + d\phi$ are, respectively, the phase shift due to sound reflection at locations x and $x + $ dx. If the phase shift gradient along the boundary is constant, Eq. (10) leads to the generalized law of reflection [18]:

$$\sin(\theta_r) - \sin(\theta_i) = n \quad \left(n = \frac{\lambda}{2\pi}\frac{d\phi}{dx}\right), \tag{11}$$

where λ is the wavelength of sound. Eq. (11) implies that the angle of reflection is no longer equal to that of incidence; that is, the reflected sound can travel in a desired direction as long as an inhomogeneous boundary impedance with a suitable constant phase gradient is provided.

Consequently, such a boundary with inhomogeneous impedance provides great flexibility in engineering the direction sound propagates. The core concept of this paper is that it is possible to make use of the surface impedance inhomogeneity to control wave reflections on the ceiling, hence guide the energy flux away from the building facade and improve the screening effect provided by the balcony.

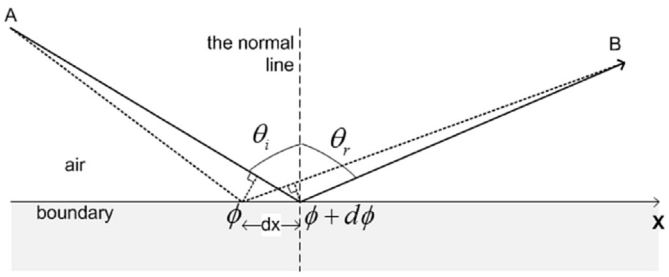

Fig. 6. Reflection of a wavefront at an inhomogeneous surface.

3.2. Theoretical analysis on a balcony with an inhomogeneous ceiling surface

In the present study, the effectiveness of the proposed treatment—a ceiling with inhomogeneous surface impedance—is investigated. It is known that the screening effect of a balcony declines for the occurrence of reflection from the ceiling. However, consider what might occur if the angle of reflection on the ceiling is made smaller than the specular reflection angle (the angle may even be negative if reflection occurs on the same side of the normal as the incident wave): in this case, sound energy will be guided away from the building facade. This anomalous reflection can be achieved if the ceiling surfaces possess appropriate surface inhomogeneities. For simplicity, here only the lossless case is considered, which means the specific impedance of the proposed ceiling surface is reactive. Similar to that adopted in Ref. [26], in this paper, the impedance of the ceiling surface is assumed to be $Z_b = -j\rho c\cot(C - \sqrt{2}kx/4)$, where C is a constant, ρ the density of air and c the speed of sound in air. For such inhomogeneous impedance, n equals $-\sqrt{2}/2$, where n is given in Eq. (11). One feature of the given inhomogeneous surface is that if sound impinges normally onto the surface the reflected angle is $-45°$.

In the previous case with a rigid-wall ceiling, using the simple geometrical relationship shown in Fig. 2, we can find that, for the reflected ray, the incident angle to the normal line of the ceiling or ground surface is $\arctan[(d+l)/(3h_0 + h_{(n)} + |y_n|)]$ $(n = 2)$, and that for the diffracted ray of order n is $\arctan[l/(h_{(n)} + |y_n|)]$ $(n = \pm 1, 2, 3, \ldots)$, where $h_{(n)}$ and y_n are given in Eq. (2). For the investigated model with the geometries listed in the caption of Fig. 1, the incident angles of these rays are all in the range of $0° < \theta_i < 45°$. Consider now that the ceiling surface is no longer rigid but with the inhomogeneous impedance $Z_b = -j\rho c\cot(C - \sqrt{2}kx/4)$. According to Eq. (11), the reflected angles of these rays will be negative and hence will occur on the same side of the normal as the incident rays. In another words, the corresponding energy flux propagates away from the building facade due to the surface inhomogeneity of the ceiling. Therefore, the sound rays that can reach the receiver $\mathbf{R_0}$ are significantly different from those in the previous rigid-wall case. In this case, as shown in Fig. 7, there are only three rays can indeed reach $\mathbf{R_0}$: the first ray diffracts at the edge of the balcony floor then reaches $\mathbf{R_0}$ (a ray with order $n = 0$); the second ray diffracts the edge of the ceiling before it reaches $\mathbf{R_0}$ (another ray with order $n = 0$); the last ray diffracts at the edge of the ceiling and then reflects on the floor before reaching $\mathbf{R_0}$ (the ray with order $n = -1$). Notice that none of

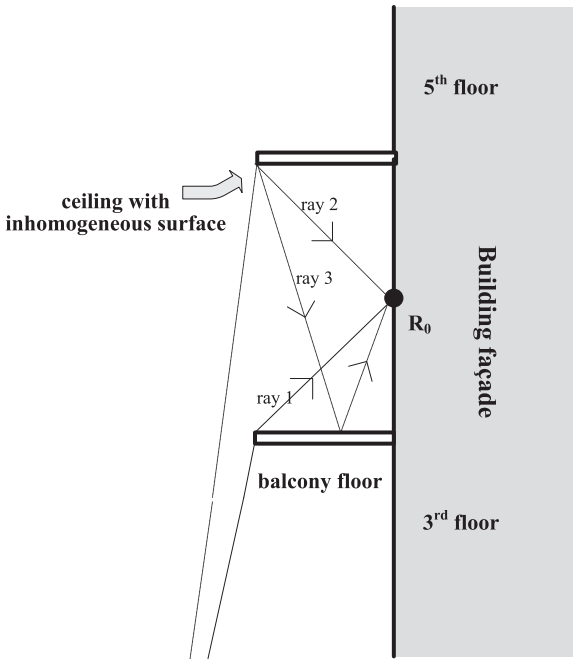

Fig. 7. Schematic representation of the three rays that can indeed reach the receiver in the case with an inhomogeneous ceiling surface.

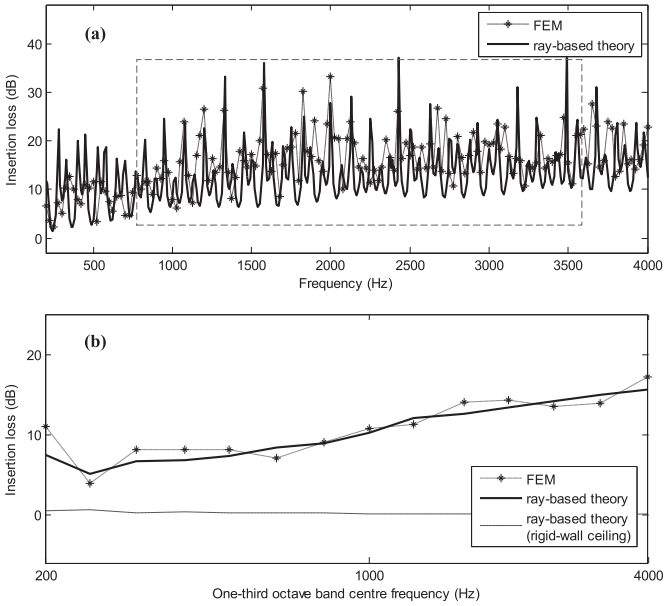

Fig. 8. (a) The spectrum of insertion losses at the receiver for the case with an inhomogeneous ceiling surface. (b) Insertion losses in one-third octave band centre frequency.

the three rays experiences any reflection on the ceiling before reaching $\mathbf{R_0}$. That is, due to the impedance inhomogeneity of the ceiling, all rays whose propagation paths include reflections on the ceiling are physically impossible to reach the receiver $\mathbf{R_0}$. In general, compared to the previous case (with a rigid-wall ceiling) that has infinite number of rays indeed reached the receiver $\mathbf{R_0}$, there are only three rays in this case. Therefore, an improvement on reducing the exterior noise from the road can be expected.

3.3. Comparison with numerical simulations for the proposed treatment with an inhomogeneous ceiling surface

The finite element modeling for the case with an inhomogeneous ceiling surface is almost the same as that adopted in the previous case with a rigid-wall ceiling, except that now the ceiling of the balcony is not rigid but with inhomogeneous impedance $Z_b = -j\rho c \cot(C - \sqrt{2}kx/4)$ along the ceiling surface. Fig. 8(a) shows the effectiveness of the proposed treatment predicted by the ray-based theory and the finite element modeling. The general trend of the IL curve, such as the positions of peaks and dips, predicted by the ray-based method coincides well with those FEM results, especially in the middle frequency range denoted by the dash-line rectangle. At low ($f < 750$ Hz) and high ($f > 3550$ Hz) frequencies, there are noticeable discrepancies for the predicted magnitudes between these two methods. These differences will be less significant if the results are averaged over a frequency range band. The comparison of IL curves in 1/3 octave band is shown in Fig. 8(b). For comparison, the IL curve predicted by the ray-based method for the conventional treatment, which is with a rigid-wall ceiling, is also plotted in Fig. 8(b). As discussed in Sec. 2, due to the reflection from the conventional ceiling, the balcony of a roadside building provides little shielding effect. However, if the ceiling possesses appropriate surface inhomogeneity, a significant improvement in insertion loss can be observed over the whole frequency range of interest. The insertion loss achieved with the proposed treatment varies from 6 to 15 dB, and the maximum insertion loss is found at 4000 Hz. In general, the overall IL, predicted by the ray-based theory and FEM simulations, are 9.6 and 11.3 dB respectively, which means that the ceiling with an inhomogeneous surface can provide effective protection against exterior traffic noise for a roadside building even when the balcony door is open.

In most part of this paper, only the balcony on the 4th story has been investigated. Fig. 9 shows the averaged ILs of balconies on different stories with the conventional and proposed treatments using the theoretical and numerical predictions. Here the receiver in each story of the building is located on the rear wall with the height $h_R = 1.5m$ above each balcony floor. The averaged IL is the decibel value of the ratio of sound energy averaged over the whole frequency range at the receiver without and with the balconies installed. In general, Fig. 9 indicates that the treatment with inhomogeneous ceiling surfaces exhibits much better noise protection than the conventional one in all stories of the building. The improvement in IL is not less than 4.7 dB and becomes greater as story increases. On the second story, the averaged IL for the conventional treatment is around 0 dB, whereas the IL for the proposed treatment is 4.7 dB. It is worth noting that, on the 4th floor, both the theoretical and numerical predictions indicate that the averaged IL for the conventional treatment is slightly below zero. This means that on the 4th story, the balcony with a rigid-wall ceiling not only has little effect in shielding the receiver from the noise source but in fact, due to the reflection from the conventional ceiling, increases the noise level. In comparison, the balcony on the 4th story with the proposed ceiling effectively reduces the noise impact on the receiver. At upper stories of the building, a significant improvement in averaged IL is achieved with the proposed treatment. For example, on the 12th floor, the numerical prediction in IL for the proposed ceiling is around 15 dB while that for the conventional one is 3 dB, an improvement of around 12 dB.

4. Realization of the proposed ceiling: a structured array of closely spaced tubes

Section 3 has shown the working principle of the ceiling whose surface has inhomogeneous impedance. So far, the inhomogeneous impedance has been arbitrarily specified as

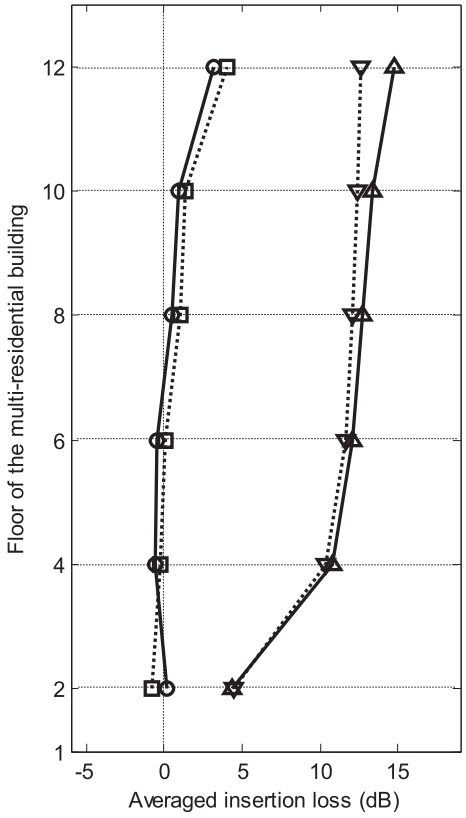

Fig. 9. The performance of balconies on different floors. ○: balconies with rigid-wall ceilings, FEM; □: balconies with rigid-wall ceilings, ray-based method, △: balconies with ceilings of inhomogeneous surfaces, FEM; ▽: balconies with ceilings of inhomogeneous surfaces, ray-based method.

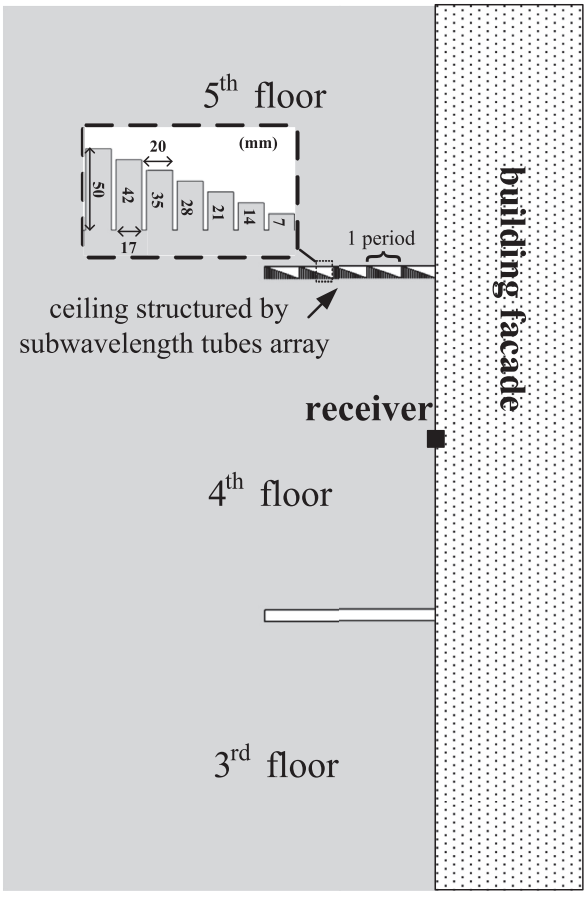

Fig. 10. Sketch of the balcony ceiling constructed of subwavelength structured tubes; inset shows the fine structure of an array. The hollow tubes are open at the end facing the balcony region and rigidly terminated at the other.

$Z_b = -j\rho c \cot(C - \sqrt{2}kx/4)$, where x is the coordinate along the ceiling surface. The form of this impedance is quite similar to that of a tube closed at one end, whose impedance is given as $Z_b = -j\rho c \cot(kl)$ [27], where l is the length of the tube. It follows, therefore, that the proposed inhomogeneous surface can be realized with a sequence of tuned tubes with spatially varying specific impedance and separated by less than a wavelength, as shown in Fig. 10. The tubes are open at the end facing the balcony region and rigidly terminated at the other. The spatially varying specific impedance is achieved by tuning the length of tubes in the array as

$$kl_n = C - \frac{\sqrt{2}}{4}kx, \tag{13}$$

where l_n is the length of the nth tube in the array. Since the wavefront manipulation requires only impedance variation along the surface, the constant C can be arbitrarily chosen so long as the condition $l_n > 0$ is ensured. However, because the thickness of the balcony must be limited for practical use, which was 0.1 m in the present study, truncation and periodization are needed in constructing the array of tubes. In this paper, the spacing between tubes in the array was set at 3 mm and their width as 17 mm, which means that even at the highest frequency of interest (4000 Hz), one wavelength will still cover 4 tubes and ensure that the surfaces are subwavelength structured.

Fig. 11 compares finite element modeling of the ideal case and its implementation via a set of tubes. It shows the ILs of the balcony with a rigid-wall ceiling, a ceiling with theoretically assigned inhomogeneous impedance, and an array of subwavelength structured tubes. It is interesting that at around 200 Hz, the balcony with the realized ceiling provides a much higher noise reduction. However, there is a considerable drop in attenuation in the low–mid frequency band (250–400 Hz): In this frequency range, theory predicts that the balcony with an inhomogeneous ceiling should have an improvement in IL of around 5–10 dB over the rigid one, but the ceiling made of an array of tubes showed less than 5 dB improvement. As discussed above, both of these phenomena are probably due to the truncation and periodization on the tube length in the array. In the mid–high frequency range, the balcony with the realized ceiling behaves quite similar to that with the ideal one (i.e. IL increases with frequency) but with a little lower

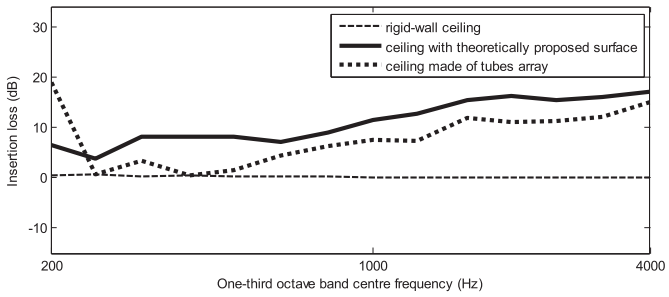

Fig. 11. Finite element modeling results of insertion loss for a balcony with a rigid-wall ceiling (dashed line), theoretically ideal ceiling (continuous line), and ceiling made of tuned tubes (dotted line).

amplitude. The FEM simulations showed the overall IL for the tube-array treatment is around 7.3 dB. In general, compared to conventional rigid-wall treatment that has little effect on providing noise protection, the subwavelength structured array of tubes offers superior environmental noise protection, particularly in the mid-–high frequency range. Moreover, it can be expected that by optimal design on the separation of tubes and periodization of the tube lengths, the performance of a balcony with closely spaced tubes, such as the drop in IL curve in the low–mid frequency band, can be further improved.

5. Discussion and conclusion

In the present study, the acoustic performance of a balcony with different types of ceiling has been investigated. A ray-based model combining the image receiver method and sound diffraction theory has been used to analysis the performance of a roadside balcony, which agreed well with numerical simulations using a two-dimensional finite element method. It is found that for a roadside building, the shielding effect provided by a balcony is significantly canceled by the reflection from the conventional ceiling. Therefore, we have proposed a novel treatment of ceiling based on inhomogeneous surface impedance. The proposed ceiling works by altering the direction of sound energy flux away from the region of the balcony as it reflects on the ceiling surface. As long as a suitable constant phase gradient along the surface is provided, the balcony with such type of ceiling offers a significant improvement in noise shielding compared to conventional one with a rigid-wall ceiling. The theoretical inhomogeneous ceiling surface has been realized in terms of a subwavelength structured array of tuned tubes, and the performance of this arrangement has been studied. The calculated performance of a balcony with the ceiling structured by the tube array has a similar performance to the proposed one in the mid-–high frequency range.

There are other acoustical components that can be formed into a structured array to achieve an inhomogeneous surface. Instead of an array of closed-end tubes, a series of Helmholtz resonators with spatially varying resonant frequencies could also be used. By spatially tailoring the geometry of the acoustical components, one can implement an impedance inhomogeneity and mold the wavefront of the reflected sound in great flexible ways. However, the major difference between the ideally proposed surface and any structured by actual acoustic component with subwavelength separation is that the latter must be discrete, and the rigid wall joining two neighboring components will be governed by conventional laws of reflection and produce the specular reflection. Furthermore, due to practical limitations on the balcony thickness, the length of tubes in the array must be truncated and periodized. Because of these factors, the ceiling structured by closely spaced components will always perform poorer than theory suggests. Therefore, as discussed above, there is a considerable drop in attenuation in the low–mid frequency band for a balcony with a ceiling structured by tubes array. In this paper, the inhomogeneous impedance has been artificially chosen as $Z_b = -j\rho c\cot(C - \sqrt{2}kx/4)$. Further systematic investigation is needed to determine how performance varies with each of the important system parameters, such as constant phase gradient of the surface impedance, separation of tubes, and periodization of the tube lengths. Once optimized, it is expected that the performance of a balcony with the ceiling structured by closely spaced acoustic components can be further improved. The present work forms a basis on which construction of actual subwavelength structured tube arrays can be done. It is hoped the present study can provide a stepping stone for investigation of more effective balcony treatments and their potential application in roadside multi-residential buildings against exterior noise.

Acknowledgment

This work was financially supported in part by the National Science Foundation of China under Grant Nos. 11304229 and 11204219, as well as the Fundamental Research Funds for the Central Universities under Grant No. 2013KJ045.

References

[1] W.H.K. Lam, M.L. Tam, Reliability analysis of traffic noise estimates in Hong Kong, Transp. Res. Part D: Transp. Environ. 3 (1998) 239–248.
[2] D.J. Kang, J.M. Kim, J.C. Park, Road traffic noise status and prediction, Trans. Korean Soc. Noise Vib. Eng. 14 (10) (2004) 1015–1020.
[3] Joint Practice Note No. 1, Green and Innovative Buildings. Hong Kong Special Administrative Region: Building Department, Lands Department and Planning Department, 2001.
[4] E.A. Mohsen, D.J. Oldham, Traffic noise reduction due to the screening effect of balconies on a building façade, Appl. Acoust. 10 (1977) 243–257.
[5] D.N. May, Freeway noise and high-rise balconies, J. Acoust. Soc. Am. 65 (1979) 699–704.
[6] D.C. Hothersall, K.V. Horoshenkov, S.E. Mercy, Numerical modeling of the sound field near a tall building with balconies near a road, J. Sound Vib. 198 (1996) 507–515.
[7] A. Cheung, K.O. Chan, K.K. Ng, Road traffic noise on balcony, in: The 6th Western Pacific Regional Acoustics Conference, 1997, pp. 32–38.
[8] W. Kropp, J. Berillon, A theoretical model to consider the influence of absorbing surfaces inside the cavity of balconies, Acta Acust. 86 (2000) 485–494.
[9] W.F. Cheng, Fung KC. NG CF, The theoretical model to optimize noise barrier performance at the window of a high-rise building, J. Sound Vib. 238 (1) (2000) 51–63.
[10] Department of Transport, Welsh Office, Calculation of Road Traffic Noise, HMSO, London, 1988.
[11] K.M. Li, W.K. Lui, K.K. Lau, K.S. Chan, A simple formula for evaluating the acoustic effect of balconies in protecting dwellings against road traffic noise, Appl. Acoust. 64 (2003) 633–653.
[12] R.N.S. Hammad, B.M. Gibbs, The acoustic performance of building façades in hot climates: Part 2—closed balconies, Appl. Acoust. 16 (1983) 441–454.
[13] H. Hossam El-Dien, P. Woloszyn, Prediction of the sound field into high-rise building facades due to its balcony ceiling form, Appl. Acoust. 65 (2004) 431–440.
[14] H. Hossam El-Dien, P. Woloszyn, The acoustical influence of balcony depth and parapet form: experiments and simulations, Appl. Acoust. 66 (2005) 533–551.
[15] S.K. Tang, Noise screening effects of balconies on a building façade, J. Acoust. Soc. Am. 118 (2005) 213–221.
[16] P.J. Lee, Y.H. Kim, J.Y. Jeon, K.D. Song, Effect of apartment building façade and balcony design on the reduction of exterior noise, Build. Environ. 42 (2007) 3517–3528.
[17] D.J. Oldham, E.A. Mohsen, A technique for predicting the performance of self-protecting buildings, Noise Control Eng. J. 15 (1) (1980) 11–19.
[18] N. Yu, et al., Light propagation with phase discontinuities: generalized laws of reflection and refraction, Science 334 (2010) 333–337.
[19] J.J. Zhao, B.W. Li, Z.N. Chen, C.W. Qiu, Manipulating acoustic wavefront by inhomogeneous impedance and steerable extraordinary reflection, Sci. Rep. 3 (2013).
[20] A. Muradali, K.R. Fyfe, A study of 2D and 3D barrier insertion loss using improved diffraction-based methods, Appl. Acoust. 53 (1998) 49–75.
[21] A.D. Pierce, Diffraction of sound around corners and over wide barriers, J. Acoust. Soc. Am. 55 (1974) 941–955.
[22] R. Panneton, A. L'Esperance, J. Nicolas, G.A. Dadigle, Development and validation of a model predicting the performance of hard or absorbent parallel noise barriers, J. Acoust. Soc. Jpn. 14 (1993) 251–257.
[23] M. Abramowitz, A. Stegun, Handbook of Mathematical Functions with Formulas, Graphs, and Mathematical Tables, Dover, New York, 1970, pp. pp.300–pp.303.
[24] J. Berenger, A perfectly matched layer for the absorption of electromagnetic waves, J. Comput Phys. 114 (1994) 185–200.
[25] Hecht E. Optics, fourth ed., Addison Wesley, New York, 2001, pp. 106–111.
[26] X. Wang, D.X. Mao, W.Z. Yu, Z.X. Jiang, Sound barriers from materials of inhomogeneous impedance, J. Acoust. Soc. Am. 137 (2015) 3190–3197.
[27] K.E. Kinsler, A.R. Frey, A.B. Coppens, J.V. Sanders, Fundamentals of Acoustics, fourth ed., Wiley, New York, 2000, pp. 150–161.